Role of the Sulfhydryl Group on the Gas Phase Fragmentation Reactions of Protonated Cysteine and Cysteine Containing Peptides

Richard A. J. O'Hair, Michelle L. Styles, and Gavin E. Reid*
School of Chemistry, University of Melbourne, Parkville, Victoria, Australia

The gas phase fragmentation reactions of protonated cysteine and cysteine-containing peptides have been studied using a combination of collisional activation in a tandem mass spectrometer and ab initio calculations [at the MP2(FC)/6-31G*//HF/6-31G* level of theory]. There are two major competing dissociation pathways for protonated cysteine involving: (i) loss of ammonia, and (ii) loss of the elements of $[CH_2O_2]$. MS/MS, MS/MS of selected ions formed by collisional activation in the electrospray ionization source as well as ab initio calculations have been carried out to determine the mechanisms of these reactions. The ab initio results reveal that the most stable $[M + H - NH_3]^+$ isomer is an episulfonium ion (**A**), whereas the most stable $[M + H - CH_2O_2]^+$ isomer is an immonium ion (**B**). The effect of the position of the cysteine residue on the fragmentation reactions of the $[M + H]^+$ ions of all the possible simple dipeptide and tripeptide methyl esters containing one cysteine (where all other residues are glycine) has also been investigated. When cysteine is at the N-terminal position, NH_3 loss is observed, although the relative abundance of the resultant $[M + H - NH_3]^+$ ion decreases with increasing peptide size. In contrast, when cysteine is at any other position, water loss is observed. The proposed mechanism for loss of H_2O is in competition with those channels leading to the formation of structurally relevant sequence ions. (J Am Soc Mass Spectrom 1998, 9, 1275–1284) © 1998 American Society for Mass Spectrometry

During our studies on the gas phase alkylation reactions of amino acids and simple peptides, we became interested in understanding the fragmention reactions of their related $[M + H]^+$ ions [1, 2]. Cysteine and its peptides are of considerable interest because the reactive thiol side chain can act as both an intermolecular [1a] and intramolecular [2] nucleophile. For example, we have shown that cysteine can be S-methylated in the gas phase [1a] and that water loss from the $[M + H]^+$ ions of N-acetyl cysteine and glycyl–cysteine can be induced by the thiol side chain (eq 1) [2]. In the former study we postulated that the two important reaction channels in the collision-induced dissociation (CID) of the $[M + CH_3]^+$ ions of cysteine result in (i), the formation of episulfonium ions (**A**) via NH_3 loss and (ii), the formation of immonium ions (**B**) via loss of the combined elements of H_2O and CO. Possible mechanisms for the competing reactions for the formation of (**A**) and (**B**) are shown in Scheme **1**.

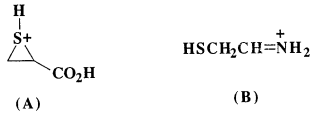

(A) (B)

The role that the site of protonation has on the fragmentation of amino acids and peptides has attracted considerable recent interest [3–8]. The initial, thermodynamically favored site of protonation may not be the species that is ultimately responsible for fragmentation. Instead, intramolecular proton transfer may be required to give a new ion that is more susceptible to bond cleavage (fragmentation). This has led to the concept of the "mobile proton model" to rationalize the competing fragmentation reactions of peptides [8]. The prototypical example is protonated glycine for which N protonation yields the thermodynamically favored species. Fragmentation of protonated glycine is, however, triggered by translocation of the proton from the protonated amino group to the OH of the carboxylic acid [cf. Path (B) in Scheme **1**], which readily fragments via loss of H_2O and CO to form the immonium ion $[H_2N{=}CH_2]^+$ [5, 7f]. Recent ab initio calculations by Uggerud [5] indicate that this intramolecular proton transfer has a relatively large transition state barrier, whereas subsequent steps leading to the loss of H_2O and CO were predicted to be less energetically demanding.

Address reprint requests to Richard A.J. O'Hair, School of Chemistry, University of Melbourne, Parkville, Victoria 3052, Australia. E-mail: r.ohair@chemistry.unimelb.edu.au

*Also at: Joint Protein Structure Laboratory, The Ludwig Institute for Cancer Research and the Walter and Eliza Hall Institute of Medical Research, P.O. Royal Melbourne Hospital, Parkville, Victoria 3050, Australia.

Presented in part at the 46th ASMS conference. This article is Part 13 of the series "Gas Phase Ion Chemistry of Biomolecules."

1044-0305/98/$19.00
PII S1044-0305(98)00104-4

Received May 7, 1998
Revised July 20, 1998
Accepted July 23, 1998

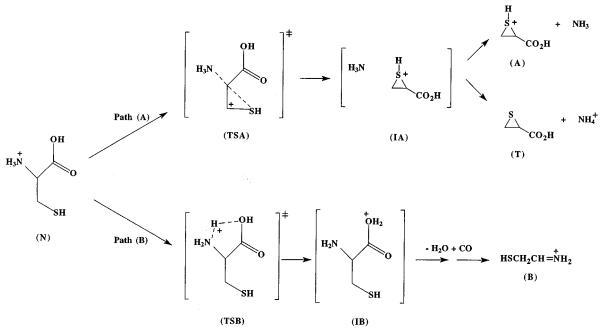

Scheme 1

The fragmentation reactions of cysteine offers a unique opportunity to examine the competition between direct fragmentation of the thermodynamically favored protonated species [Path (A) in Scheme **1**] versus proton transfer to an isomeric, less favored protonated species prior to fragmentation [Path (B) in Scheme **1**]. A further point of interest is the direct solution phase analogy to the gas phase loss of ammonia from cysteine, leading to the formation of the episulfonium ion (**A**) [Path (A) in Scheme **1**]. For example, cysteine and its esters undergo deaminative cyclizations to give thiiranecarboxylic acids when treated with sodium nitrite–hydrochloric acid (eq 2) [9]. In this case, the amino group of cysteine is converted into a better leaving group (N_2), thereby facilitating this cyclization reaction.

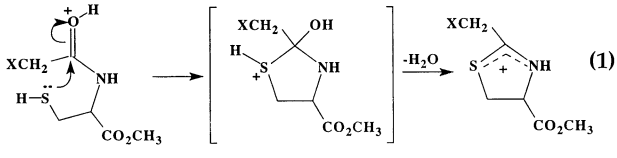

(1)

In this article we examine: (i) the fragmentation reactions of protonated cysteine under MS/MS and "in source" CID MS/MS (hereafter designated as sCID/MS/MS) conditions in both triple quadrupole and quadrupole ion trap mass spectrometers [10], (ii) the mechanisms for the formation of (**A**) and (**B**) via ab initio calculations [11–14], (iii) whether loss of NH_3 is a general CID reaction of $[M+H]^+$ ions for cysteine containing peptides in which the cysteine residue is at the N-terminus, and (iv) the influence of the reactive nucleophilic sulfhydryl side chain of cysteine on the formation of structurally relevant "sequence" ions.

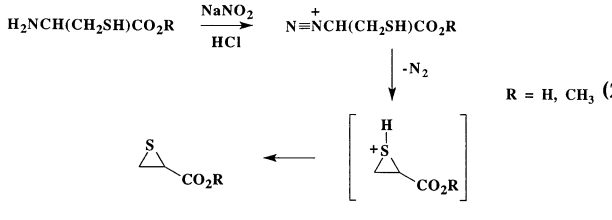

R = H, CH_3 (2)

Experimental

Methods

Cysteinyl–glycyl–glycine was synthesised using automated rapid SPPS methodologies on an Applied Biosystems (Foster City, CA) model 430A peptide synthesizer as previously described [15]. The thiirancarboxylic acid methyl ester was prepared according to a literature procedure and was used without further purification [9]. Amino acid and peptide methyl esters were prepared as described previously [2]. All other reagents were commercially available and were used without further purification. D_2-cysteine [$H_2NCH(CD_2SH)CO_2H$ (98% D)] was obtained from Cambridge Isotope Laboratories (Andover, MA).

Mass Spectrometry

Protonated cysteine $[M+H]^+$ ions were formed via electrospray ionization (ESI) on either: (i) a Finnigan TSQ-700 (San Jose, CA) triple quadrupole mass spectrometer or (ii) a Finnigan model LCQ quadrupole ion trap mass spectrometer. Samples, (0.1 mg/mL) dissolved in 50% methanol/50% H_2O containing 0.1 M acetic acid were introduced to the mass spectrometer at 2 μL/min via a length of 190 μm outside diameter $\times$ 50 μm internal diameter fused silica tubing. The spray voltage was set at -5 kV. Nitrogen sheath gas was supplied at 30 lb/in^2. The heated capillary temperature was 200° C. In the triple quadrupole mass spectrometer, MS/MS was performed by CID of selected ions. The argon collision gas pressure was maintained at 2–2.5 mtorr. The collision energy was incremented in steps of 2.5 eV (laboratory frame of reference) from 5 to 30 eV. "In-source" CID (sCID) in the tube–lens/skimmer region of the ESI source (+ 30 V) was performed with subsequent CID of selected product ions in the rf only collision cell of the mass spectrometer. MS/MS experiments were performed on mass selected ions in the quadrupole ion trap mass spectrometer using standard isolation and excitation procedures.

Computational Methods

Structures of minima and transition states were optimized at the Hartree–Fock level using the following molecular modeling packages: GAMESS [11], GAUSSIAN 94 [12], and Spartan (Ver 5.0) [13] with the standard 6-31G* basis set [14]. All optimized structures were then subjected to vibrational frequency analysis to determine the nature of the stationary points, followed by a single point energy calculation of the correlated energy at the MP2(FC)/6-31G* level of theory (FC = frozen core). Energies were corrected for zero-point vibrations scaled by 0.9135 [16]. Intrinsic reaction coordinate (IRC) runs were performed on each transition

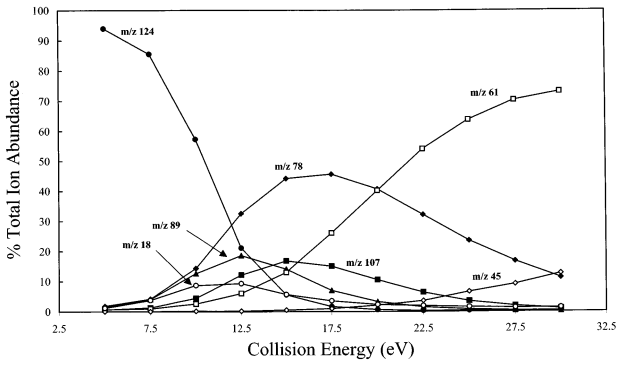

Figure 1. Energy resolved CID of the $[M+H]^+$ ion of D_2-cysteine. See Experimental section for details. Filled circle—m/z 124, filled square—m/z 107, filled triangle—m/z 89, filled diamond—m/z 78, open square—m/z 61, open diamond—m/z 45, open circle—m/z 18.

state to check that they connected to the appropriate minima. Complete structural details and lists of vibrational frequencies for each HF/6-31G* optimized structure are available from the office of the Editor of *J. Am. Soc. Mass Spectrom.*

Results and Discussion

MS/MS Studies on the $[M+H]^+$ Ion of Cysteine

The fragmentation reactions of the $[M+H]^+$ ion of cysteine and D_2-cysteine were studied as a function of collision energy using the triple quadrupole instrument (D_2-cysteine was used to help assign fragment ions). Figure 1 demonstrates the dependence of collision energy on fragment ion yield (expressed as a percentage of the total ion abundance for each collision energy value) for the $[M+H]^+$ ion of D_2-cysteine. At low collision energies (<12.5 eV), the primary fragmentations observed corresponded to eqs 3–5 (consistent with the proposed mechanisms shown in Scheme **1**). It is clear from the data in Figure 1 that the onset of ions at higher collision energies results from the secondary fragmentation of daughter ions generated at low collision energy values. Thus, at higher collision energies (>12.5 eV), a new fragmentation channel was observed corresponding to eq 6. At the highest collision energy studied (30 eV), two additional secondary fragmentation products were observed (eq 7 and 8). The latter reaction is noteworthy since it involves homolytic cleavage of $HS^{\cdot}$ to yield the radical cation $[CD^2CHNH_2]^{+\cdot}$.

$$[H_2NCH(CD_2SH)CO_2H + H]^+ \rightarrow [HSCD_2CHCO_2H]^+ + NH_3\ m/z\ 107 \quad (3)$$

$$[H_2NCH(CD_2SH)CO_2H + H]^+ \rightarrow NH_4^+ + [SCD_2CHCO_2H]\ m/z\ 18 \quad (4)$$

$$[H_2NCH(CD_2SH)CO_2H + H]^+ \rightarrow [HSCD_2CHNH_2]^+ + H_2O + CO\ m/z\ 78 \quad (5)$$

$$[H_2NCH(CD_2SH)CO_2H + H]^+ \rightarrow [SCD_2CHCO]^+ + NH_3 + H_2O\ m/z\ 89 \quad (6)$$

$$[H_2NCH(CD_2SH)CO_2H + H]^+ \rightarrow [SCD_2CH]^+ + NH_3 + H_2O + CO\ m/z\ 61 \quad (7)$$

$$[H_2NCH(CD_2SH)CO_2H + H]^+ \rightarrow [CD_2CHNH_2]^{+\cdot} + H_2O + CO + HS^{\cdot}\ m/z\ 45 \quad (8)$$

In the LCQ, fewer fragmentation reactions were observed upon collisional activation of the $[M + H]^+$ ion of cysteine. Indeed the only two products are those shown in eqs 3 and 5, which were formed in an approximate ratio of 2:1.

These results compare favorably with previous MS/MS studies on the fragmentation of the $[M + H]^+$ ion of cysteine. For example, Kulik and Herma [4a] carried out MS/MS on fast atom bombardment generated ions and found dominant loss of NH_3 and minor losses of H_2O and (H_2O + CO), whereas Harrison and co-workers [4b] showed that under low energy CID conditions, the exclusive loss of NH_3 at low collision energies and increasing amounts of H_2O + CO loss at higher collision energies was observed. Additionally, Harrison et al. demonstrated that the $[M + H - NH_3]^+$ ion fragmented further by loss of H_2O and the $[M + H - H_2O + CO]^+$ ion fragmented by loss of NH_3 and suggested that the $[M + H - NH_3]^+$ ion was stabilized by "anchimeric assistance by the sulfur substituent." Neither group however, provided any detailed discussion of the potential structures of the resultant product ions or predicted possible mechanisms for the two major (primary) fragmentation reactions.

To obtain further insights into the structures of the product ions as well as the mechanisms for formation of the two major fragmentation reactions of protonated cysteine (eqs 3 and 5), both sCID/MS/MS studies and ab initio calculations were performed. These results are presented in the following sections.

sCID/MS/MS and Ab Initio Studies on Possible Structures for the $[M + H - NH_3]^+$ and $[M + H - H_2CO_2]^+$ Product Ions of Cysteine

The ms/ms spectrum of the $[M + H]^+$ ion of cysteine is shown in Figure 2A. In order to probe the structures of the $[M + H - NH_3]^+$ and $[M + H - H_2CO_2]^+$ ions, and to determine the origin of the other product ions in the spectrum, the potential of the tube-lens voltage in the high pressure source region of the electrospray ionization interface was increased by +30 V to induce sCID fragmentation. Selected product ions were then isolated and subjected to CID in the octapole collision cell.

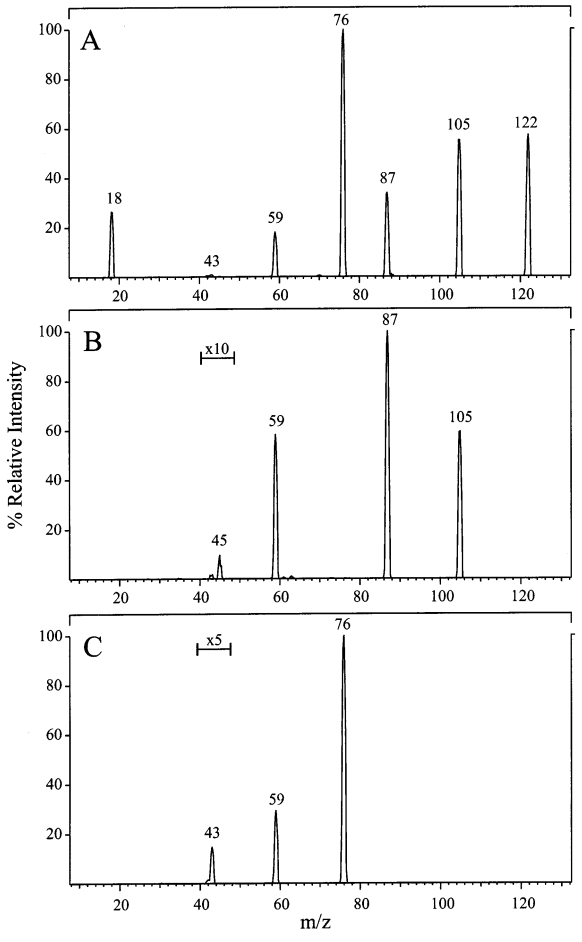

Figure 2. Triple quadrupole (12.5 eV, laboratory frame of reference) MS/MS spectrum of (**a**) the $[M + H]^+$ ion and the sCID/MS/MS spectra of (**b**) the $[M + H - NH_3]^+$ and (**c**) the $[M + H - H_2CO_2]^+$ ions of protonated cysteine. See Experimental section for details.

Examination of the sCID/ms/ms product ion spectrum of the $[M + H - NH_3]^+$ ion (m/z 105) of cysteine, formed via collisional activation in the ESI source of the triple quadrupole mass spectrometer (Figure 2B) revealed loss of H_2O (m/z 87) (cf. eq 6), (H_2O + CO) (m/z 59) (cf. eq 7) and minor formation of an ion at m/z 45. The sCID/ms/ms product ion spectrum of the $[M + H - H_2CO_2]^+$ ion (m/z 76) of cysteine (Figure 2B) revealed loss of NH_3 as the major fragmentation product. A minor ion (m/z 43) corresponding to the loss of HS˙ was also observed (cf. eq 8).

What can we infer from these experiments? The loss of H_2O and the combined elements of H_2CO_2 (H_2O + CO) for the $[M + H - NH_3]^+$ ion of cysteine are indicative of an ion containing a carboxylic acid functional group [1a–c], which is consistent with an ion of structure (**A**). Similarly, losses of NH_3 and HS˙ from the $[M + H - H_2CO_2]^+$ ion of cysteine are consistent with an ion of structure (**B**).

To obtain further evidence that the $[M + H - NH_3]^+$ ion of cysteine forms the episulfonium ion (**A**), we synthesized the related neutral thiiranecarboxylic acid methyl ester via a solution phase sodium nitrite–hydrochloric acid deamination reaction (eq 2) [5]. MS/MS of the protonated product (m/z 119) resulted in the loss of CH_3OH and (CH_3OH + CO) (Table 1). The product ions observed and the relative yields compared favorably with those seen in the sCID/MS/MS product ion spectrum of the $[M + H - NH_3]^+$ ion of cysteine methyl ester (Table 1).

Although the sCID/MS/MS spectra were consistent with structures (**A**) and (**B**) for the $[M + H - NH_3]^+$ and $[M + H - H_2CO_2]^+$ fragment ions of cysteine, a number of other isomeric structures are possible. In order to gain insights into the stabilities of some of these isomeric ions in the gas phase, we have turned to ab initio calculations, focusing on five different structures (**A**), (**C**)–(**F**) for the $[M + H - NH_3]^+$ ion and four different structures (**B**), (**G**)–(**I**) for the $[M + H - H_2CO_2]^+$ ion. Thus we have ignored isomers for which complex skeletal rearrangements are required.

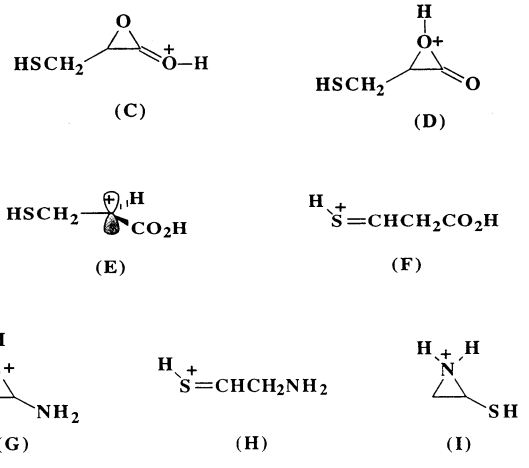

Table 1. Triple quadrupole mass spectrometric sCID/MS/MS of the $[M+H]^+$ ions of cysteine derivatives

Parent species	sCID product ion[a]	m/z	MS/MS product ions,[b] m/z (loss), % abundance[c]
D_2-cysteine	$[M + H - H_2CO_2]^+$	78	61 (NH_3) 84, 45 (NH_3 + SH) 14
D_2-cysteine	$[M + H - NH_3]^+$	107	89 (H_2O) 70, 61 (H_2O + CO) 100
Cysteine–OMe	$[M + H - NH_3]^+$	119	87 (CH_3OH) 100, 59 (CH_3OH + CO) 64
Thiiranecarboxylic acid–OMe[d]	—	119	87 (CH_3OH) 100, 59 (CH_3OH + CO) 42

[a]Formed by ESI-in source CID.
[b]MS/MS in collision cell at a collision energy of 12.5 eV.
[c]Ions of less than 1% abundance are not shown.
[d]Formed by ESI-MS.

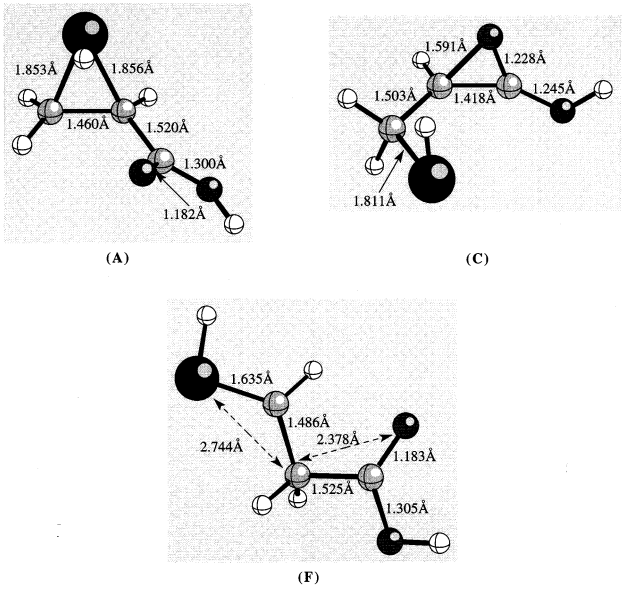

Figure 3. HF/6-31G* optimized geometries of various isomeric $[M+H - NH_3]^+$ ions.

Structures of type (**A**) result from loss of ammonia via neighboring group participation by the sulfhydryl group, whereas those of (**C**) and (**D**) involve neighboring group participation by the C=O oxygen atom and the HO oxygen atom of the carboxyl group respectively [17]. Direct loss of ammonia results in the formation of the secondary carbocation (**E**), whereas a 1,2 hydride transfer from (**E**) would yield the resonance stabilized ion (**F**). Ab initio calculations were carried out on each of these structures [18].

Four different stable minima were located on the HF/6-31G* potential energy surface for (**A**), whereas two conformers were found for both (**C**) and (**F**). Structure (**D**) was not stable, undergoing ring opening to form an acylium ion (**J**). The secondary carbocation, (**E**), does not appear to be a stable minimum at the HF/6-31G* level of theory. All attempts to optimize such a structure either with or without the imposition of symmetry constraints resulted in ring closure to form structure (**A**). The most stable minima for each of (**A**), (**C**), and (**F**), are shown in Figure 3 and their energies are reported in Table 2. Note that at the MP2(FC)/6-31G*//HF/6-31G* level of theory, the episulfonium ion (**A**) is predicted to be the most stable species, followed by (**F**) (+ 2.9 kcal mol^{-1}). Species (**C**) is predicted to be 36.8 kcal mol^{-1} less stable than (**A**), suggesting that the $-CO_2H$ group is a poorer neighboring group than –SH. (Neighboring group participation involves intramolecular nucleophilic attack at a reaction center, often followed by displacement of a leaving group with the formation of a cyclic product. In evaluating the relative neighboring group participation ability of two different groups, both the inherent nucleophilicity of the groups as well as the stability of the resultant ring are factors. For a discussion see [17].)

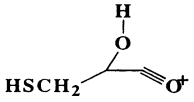

(**J**)

Structures (**B**), (**G**), (**H**), and (**I**) were examined as possible candidates for the $[M + H - H_2CO_2]^+$ fragment ion. Two stable conformers were located for (**B**), whereas only one stable structure was found for (**I**) (Figure 4). Structures (**G**) and (**H**) were both unstable at the HF/6-31G* level of theory and yielded (**B**) and (**I**),

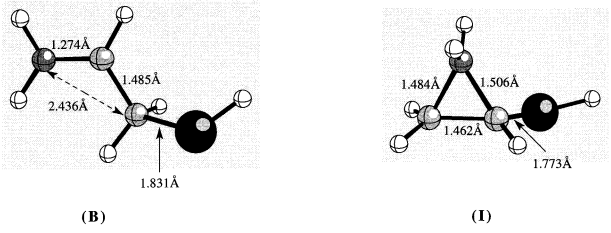

Figure 4. HF/6-31G* optimized geometries of various isomeric $[M + H - H_2CO_2]^+$ ions.

Table 2. Ab initio total energies and zero point vibrational energies of the isomeric $[M + H - NH_3]^+$ and $[M + H - H_2CO_2]^+$ ions of cysteine

	Energies (hartrees)		Relative energies[c] (kcal mol^{-1})	
Species[a]	HF/6-31G*	MP2[b]	ZPVE[d]	MP2[e]
$[M + H - NH_3]^+$ ions				
(**A**)	−663.47176	−664.32293	0.07945	0.0
(**C**)	−663.41705	−664.26236	0.07772	36.8
(**F**)	−663.47699	−664.31677	0.07817	2.9
$[M + H - H_2CO_2]^+$ ions				
(**B**)	−530.94167	−531.46620	0.08147	0.0
(**I**)	−530.91177	−531.44645	0.08282	13.2

[a]See text for structures.
[b]At the MP2(FC)/6-31G*//HF/6-31G* level of theory.
[c]Relative to the most stable $[M + H - NH_3]^+$ or $[M + H - H_2CO_2]^+$ ions, respectively.
[d]Corrected by 0.9135 [12].
[e]At the MP2(FC)/6-31G*//HF/6-31G*+0.9135 ZPVE level of theory.

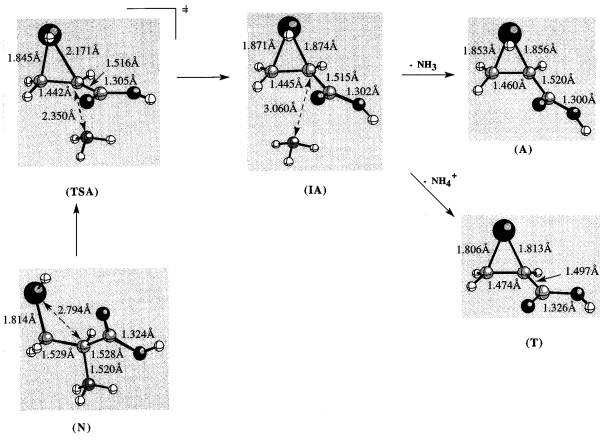

Figure 5. HF/6-31G* optimized geometries of species associated with formation of the episulfonium ion (**A**).

respectively, upon optimization. (**B**) is predicted to be more stable than (**I**) by over 13 kcal mol^{-1} (Table 2).

Given that the ab initio calculations indicated that (**A**) and (**B**) are the most stable structures for the $[M + H - NH_3]^+$ and $[M + H - H_2CO_2]^+$ fragment ions of protonated cysteine, we have examined the potential energy surface for the formation of these ions at the HF/6-31G* level of theory.

Ab Initio Studies on the Reaction Coordinates for the Formation of the $[M + H - NH_3]^+$ and $[M + H - H_2CO_2]^+$ Product Ions of Cysteine

Our results from above suggest that the most likely structures of the $[M + H - NH_3]^+$ and $[M + H - H_2CO_2]^+$ ions are (**A**) and (**B**), respectively. Given the numerous conformations for the various isomers of protonated cysteine, we have focused on finding the transition state that yields the most stable conformer of the episulfonium ion (**A**). An initial "guess" for this transition state (**TSA**) was optimized at the AM1 level of theory, and then reoptimized at the HF/6-31G* level of theory. Vibrational frequency analysis confirmed that (**TSA**) had an imaginary frequency of 368.13i cm^{-1} at the HF/6-31G* level of theory, which corresponds to the intramolecular displacement of NH_3 by the sulfhydryl group [19]. The hessian from the vibrational frequency analysis of (**TSA**) was then used to perform an intrinsic reaction coordinate search to locate the starting reactant [(**N**), a conformer of N-protonated cysteine] and the intermediate (**IA**), which is an ion–molecule complex [20] between ammonia and the episulfonium ion. Dissociation of this ion–molecule complex (**IA**) yields (**A**) plus neutral NH_3, whereas proton transfer prior to dissociation yields the neutral thiirane (**T**) together with NH_4^+. Each of the structures of these HF-6-31G* optimized species are shown in Figures 3 and 5, whereas their energies at the MP2(FC)/6-31G*//HF/6-31G* level of theory are given in Tables 2 and 3.

Given that Uggerud [5] has shown that the key transition state for the loss of H_2O and CO from N-protonated glycine involves intramolecular proton transfer from the amino group to the OH group, we have focused on the analogous transition state for cysteine. Taking the initial structure of N-protonated cysteine found for the episulfonium ion reaction channel, a "guess" was made for the appropriate intramolecular proton transfer transition state and this structure

Table 3. Ab initio total energies and zero point vibrational energies for transition states, intermediates, and products for the formation of (**A**) and (**B**)

	Energies (hartrees)		Relative energies[c] (kcal mol^{-1})	
Species[a]	HF/6-31G*	MP2[b]	ZPE[d]	MP2[e]
N-protonated cysteine (**N**)	−719.72138	−720.74047	0.12116	0.0
Episulfonium channel				
(**TSA**)	−719.67037	−720.69382	0.11605	26.1
(**IA**)	−719.67583	−720.69900	0.11567	22.6
(**A**)	−663.47176	−664.32293	0.07945	35.2[f]
(**T**)	−663.16235	−664.01716	0.07000	13.4[g]
NH_3	−56.18436	−56.35372	0.03380	
NH_4^+	−56.53077	−56.69954	0.04867	
Immonium channel				
(**TSB**)	−719.65759	−720.68675	0.11528	30.0
(**IB1**)	−719.65787	−720.68448	0.11673	32.3
(**B**)	−530.94167	−531.46620	0.08147	29.3[h]
H_2O	−76.01075	−76.19595	0.02100	
CO	−112.73788	−113.01802	0.00508	

[a]See text for structures.
[b]At the MP2(FC)/6-31G*//HF/6-31G* level of theory.
[c]Relative to N-protonated cysteine.
[d]Corrected by 0.9135 [12].
[e]At the MP2(FC)/6-31G*//HF/6-31G*+0.9135 ZPE level of theory.
[f]The energy of NH_3 has been added
[g]The energy of NH_4^+ has been added
[h]The energy of H_2O and CO has been added.

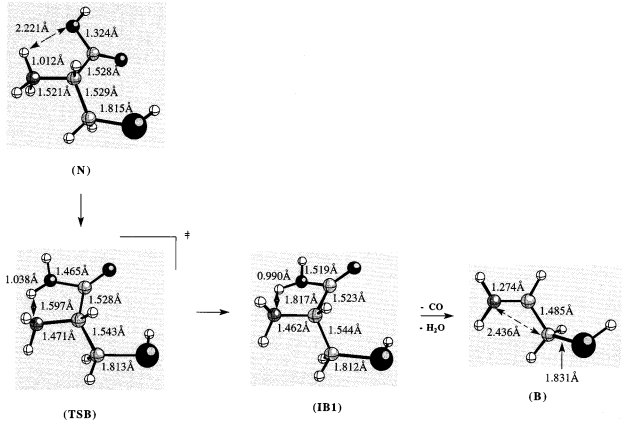

Figure 6. HF/6-31G* optimized geometries of species associated with formation of the immonium ion (**B**).

optimized. Vibrational frequency analysis confirmed that (**TSB**) had an imaginary frequency of 401.12i cm^{-1} at the HF/6-31G* level of theory, which corresponds to the intramolecular proton transfer from the N-protonated cysteine isomer (**N**) to OH protonated cysteine. The hessian from the vibrational frequency analysis of (**TSB**) was then used to perform an intrinsic reaction coordinate search to locate the starting reactant [(**N**), the same conformer of N-protonated cysteine found from **TSA**] and the intermediate (**IB**), corresponding to OH protonated cysteine. The final ionic product, the immonium ion (**B**), was optimized by removing H_2O and CO from the intermediate (**IB**). The structures of each of these HF/6-31G* optimized species are shown in Figures 4 and 6, whereas their energies at the MP2(FC)/6-31G*//HF/6-31G* level of theory are given in Tables 2 and 3.

How does the ab initio data on the energetics of the transition states and final products relate to the experimentally observed fragment ion abundances? Examination of Table 4 reveals that all three reaction channels are endothermic, the least being the formation of NH_4^+ and the neutral thiirane (eq 4). However, this ion was observed as the minor product in the triple quadrupole experiment and was not observed in the LCQ ion trap mass spectrometer (there are two possible explanations for the differences between the two instruments: (i) the inherent limitations in trapping low mass-to-charge ratio product ions in the LCQ might preclude the observation of NH_4^+; (ii) the lifetime of the ion–molecule complex may be different in both instruments [21]). Both this product and the related episulfonium ion product (eq 3) arise from the same transition state, which is predicted to be lower in energy by (3.9 kcal mol^{-1}) than the transition state corresponding to the immonium ion channel (eq 5). The relative ion abundances in the MS/MS spectrum of protonated cysteine reflect these relative barrier heights in both the triple quadrupole and LCQ ion trap mass spectrometric experiments, where the products from the episulfonium ion channels (eqs 3 and 4) were formed in higher yield than those from the immonium ion channel (eq 5).

MS/MS Studies on the Fragmentation Reactions of Some Protonated Peptides Containing Cysteine

A number of different methods have been used to examine the fragmentation mechanisms of protonated peptides, including: (i) the use of deuterium labeling [22]; (ii) the synthesis of derivatives such as methyl esters [23]; (iii) neutral fragment reionization [6d, 7b, g]; and (iv) examining the dependence of fragment ions on the internal energy of the $[M + H]^+$ ion [24]. Unfortunately, these methods have generally not been applied in a systematic way to examine the influences of different amino acid residues in dipeptides and tripeptides on the formation of various product ions. A few studies have, however, examined MS/MS spectra of the $[M + H]^+$ ions of sets of peptides [25], including dipeptides and tripeptides under similar MS/MS conditions. Of these studies, those by Kulik and Herma [6b, 7a], Isa et al. [6c], and Morgan and Bursey [7c, d] provide the largest data sets.

Isa et al. [6c] have examined the MS/MS spectra of a series of protonated dipeptides, Xxx–Gly; Gly–Xxx; Xxx–Leu; Leu–Xxx (where Xxx represents various amino acid residues), and have provided interesting insights into the formation of the a_1 versus y_1 ions [26]. For Gly–Xxx, the y_1 ions were always observed, as was the a_1 ion. In contrast, the y_1 ion was rarely seen for Xxx–Gly, where the a_1 ion usually dominated. When Gly was substituted for Leu, the abundances of the a_1 ion increased for Leu–Xxx, as did the abundances of the y_1 ion for Xxx–Leu. These results suggested that the proton affinity (PA) differences between the conjugate bases of the a_1 and y_1 ions may play a role in the relative abundances of the a and y_1 ions.

Morgan and Bursey [7c, d] have carried out a detailed analysis of the relative ratios of fragment ion

Table 4. Comparison of energetics versus fragment ion yields for the fragmentation reactions of protonated cysteine

Reaction channel	ΔE^0_{react} [a]	$\Delta E^{\ddagger}$ [a]	% abundance in LCQ	% abundance in QQQ[b]
Episulfonium ion (**A**)	+35.2	+26.1	100	85
Thiiranecarboxylic acid (**T**)	+13.4	+26.1	· · ·	25
Immonium ion (**B**)	+29.3	+30.0	50	100

[a]kcal mol^{-1}. Calculated at the MP2(FC)/6-31G*//HF/6-31G*+0.9135 ZPE level of theory.
[b]At 12.5 eV (laboratory frame of reference). Calculated by summing ion abundances of (**A**) plus fragments derived from (**A**) and comparing these to the sum of ion abundances of (**B**) plus fragments of (**B**).

Table 5. LCQ CID MS/MS of the $[M+H]^+$ ions of the methyl esters of several cysteine containing peptides

Peptide ester	Nonsequence ions[a,b]			Sequence ions[a–c]			Other fragment ions (neutral loss) % abundance
	NH_3 loss	CH_3OH loss	H_2O loss	y_1	y_2	b_2	
CG–OMe	100	2	···	4	N/A	N/A	(NH_3,CH_3OH) 1
GC–OMe[d]	···	1	100	1	N/A	N/A	···
GGG–OMe	···	8	···	100	···	79	(NH_3, CO) 3, a_2, 2
CGG–OMe	6	7	···	21	3	100	(NH_3, CO) 5
GCG–OMe	···	1	58	6	···	100	a_2, 1
GGC–OMe	···	1	100	14	···	···	···

[a]Nonsequence and sequence ions were catagorized according to the site of cleavage. Only those ions formed by amide bond cleavage are termed sequence ions. Fragment ion yields are expressed as a % abundance. Ions of less than 1% abundance are not shown.
[b](N/A), nonapplicable; (···), ion was not observed.
[c]Sequence ions are labeled according to accepted nomenclature schemes [18].
[d]Data cited from [2].

formation in the MS/MS spectra of a series of protonated tripeptides Gly–Gly–Xxx, Xxx–Gly–Gly, and Gly–Xxx–Gly (where Xxx represents various amino acid residues). They found a linear relationship between the log of the ratio of the ion abundances of the y_1 ions versus the b_2 ions and the proton affinities of the C-terminal amino acid substituents in the peptides series Gly–Gly–Xxx. Thus, as the PA of the C-terminal amino acid substituent increases, the fraction of y_1 ion formation increases [7c]. An inverse relationship between the y_2 ion abundances and the PA affinity of the N-terminal residue however, was found for the peptides series Xxx–Gly–Gly. Thus, as the PA affinity of the N-terminal residue increases, the fraction of y_2 ion decreases [7d].

To examine the effect of a nucleophilic sulfhydryl side chain on the fragmentation reactions of protonated di- and tripeptides containing cysteine (which seem to have been neglected in the literature), we have performed MS/MS experiments on the $[M+H]^+$ ions of the methyl ester derivatives of cysteinyl–glycine (CG–OMe) (m/z 193), glycyl–cysteine (GC–OMe) (m/z 193) [2], cysteinyl–glycyl–glycine (CGG–OMe) (m/z 250), glycyl–cysteinyl–glycine (GCG–OMe) (m/z 250) and glycyl–glycyl–cysteine (GGC–OMe) (m/z 250). The results of these MS/MS experiments are listed in Table 5. In addition, the MS/MS spectrum of the $[M+H]^+$ ion of GGG–OMe was also examined to determine the relative role of the position and PA of the cysteine residue on the formation of the various product ions.

The fragmentation of CG–OMe was similar to that of the methyl ester of protonated cysteine, where loss of NH_3 was observed as the major fragmentation reaction (cf. eq 3). For CGG–OMe, the major product ions observed corresponded to cleavage of the glycyl–glycyl amide bond, thus generating the complementary "sequence" ions, b_2 and y_1 [26]. In addition, a number of ions corresponding to the y_2 ion and the "nonsequence" losses of CH_3OH, NH_3, and (NH_3+CO) were also observed, albeit at low abundance. The relative yields for the fragmentation of CGG–OMe compare favorably with the general trends proposed by Morgan and Bursey [7d].

In contrast to CGG–OMe, where a complete set of sequence ions were observed (i.e., y_1, y_2, b_2 ions), both GCG–OMe and GGC–OMe exhibited incomplete sequence ion formation and a dominant nonsequence ion corresponding to the loss of H_2O (Table 5). Clearly, the position of the cysteine amino acid residue in the peptide sequence is critical to the formation of sequence and nonsequence ions. It is interesting to speculate that the absence of a b_2 ion, the low yield of the y_1 ion compared to GGG–OMe and the dominant H_2O loss in the MS/MS of the $[M + H]^+$ ion of GGC–OMe may be because of the direct competition between two neighboring groups, the adjacent carbonyl oxygen [Path (C) in Scheme **2**] versus the sulfhydryl group [Path (D) in Scheme **2**], attacking the same protonated species. If this were the case, then the relative fragment ion intensities observed would be expected to reflect the relative neighboring group abilities.

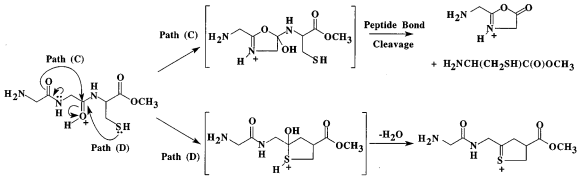

Scheme 2

In addition to the mechanism proposed previously for the loss of H_2O from GC–OMe, as previously discussed, (eq 1) [2] (see also Table 5) the dominant loss of H_2O from the tripeptides GCG–OMe and GGC–OMe could also conceivably be because of nucleophilic attack by the N-terminal amino group at the protonated carbonyl of the second amide bond (eq 9), forming a six-membered cyclic product. To determine if the loss of H_2O from GCG–OMe and GGC–OMe could be attributed to the latter reaction, the MS/MS of GGG–OMe was examined. This simplest of tripeptides should also show H_2O loss if such a process was to occur (eq 9). Examination of the data listed in Table 5 for the MS/MS of the $[M + H]^+$ ion of GGG–OMe reveals that no water loss was observed. Thus, the dominant loss of H_2O from

GCG–OMe and GGC–OMe is most likely because of the intramolecular nucleophilic attack process discussed

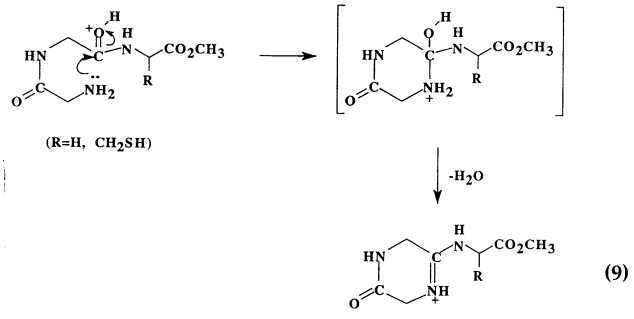

(9)

above (cf. eq 1).

Although much of the attention on the mechanisms of MS/MS fragmentation has focused on the influence of the site(s) of protonation, other factors are emerging as being important. Examples include the conformation of the ion [27] as well as the ability of various functional groups within the peptide to act as nucleophiles. The latter effect can have several consequences; the nucleophilic group can: (i) help "solvate" the charge site; (ii) act as a proton shuttle (i.e., to transfer the proton from one site to another in an intramolecular fashion); or (iii) help induce cleavage (thereby acting as a neighboring group participant) [7]. Note that whenever the nucleophile acts as a neighboring group, it ends up being part of a ring system (cf. eqs 1, 2, and 9). The notion that a neighboring group may help trigger a cleavage reaction is slowly gaining acceptance [4b, 7e, 7e, 28, 29]. For example, the formation of oxazolones suggests that peptide bond cleavage is triggered by the adjacent carbonyl oxygen atom [7e] [Path (C) in Scheme **2**]. Additionally, the side chain of aspartic acid has been shown to help enhance the cleavage of adjacent peptide bonds (via a proposed mechanism involving nucleophilic attack by the side chain) [28], whereas the α- and ε-amino groups of protonated lysine [29] have been implicated in fragmentation reactions by neighboring group participation.

Conclusions

Using a combination of collisional activation in a tandem mass spectrometer, sCID/MS/MS experiments and ab initio calculations [at the MP2(FC)/6-31G*//HF/6-31G* level of theory], we have demonstrated that the two major competing dissociation pathways for protonated cysteine involving: (i) loss of ammonia, with concomitant formation of a $[M + H - NH_3]^+$ ion and (ii) loss of the elements of $[CH_2O_2]$ result in the formation of episulfonium (**A**) and immonium ions (**B**), respectively. The transition state for formation of the episulfonium ion product (**A**) was predicted to be slightly lower in energy (3.9 kcal mol^{-1}) than the transition state corresponding to the immonium ion (**B**). The relative ion abundances in the MS/MS spectrum of protonated cysteine reflect these relative barrier heights in both triple quadrupole and LCQ ion trap mass spectrometric experiments.

The position of the cysteine residue has been shown to have a dramatic influence on the fragmentation reactions of the $[M + H]^+$ ions of cysteine containing peptides. When cysteine was at the N-terminal position, NH_3 loss was observed, although the relative abundance of the resultant $[M + H - NH_3]^+$ ion decreased with increasing peptide size. In contrast, H_2O loss was observed when cysteine was at any other position. This dominant H_2O loss and the lack of structurally relevant sequence ions in the MS/MS of the $[M + H]^+$ ion of GGC–OMe may be because of the direct competition between two neighboring groups, the adjacent carbonyl oxygen and the sulfhydryl group, attacking the same protonated species. Further studies are currently underway to assess the role of other side chains in the fragmentation reactions of peptide $[M + H]^+$ and $[M + nH]^{n+}$ ions.

Supplementary Material

Supplementary material for this article is available in photocopy form from the office of the Editor-in-Chief (see inside front of journal for address). Requests must include complete title of article, names of authors, issue date, and page numbers.

Acknowledgments

RAJO thanks the ARC for financial support and the University of Melbourne for funds to purchase the LCQ. MLS and GER acknowledge the award of Commonwealth Postgraduate Scholarships.

References

1. (a) Freitas, M. A.; O'Hair, R. A. J.; Williams, T. D. *J. Org. Chem.* **1997,** *62,* 6112–6120. (b) O'Hair, R. A. J.; Freitas, M. A.; Gronert, S.; Schmidt, J. A. R.; Williams, T. D. *J. Org. Chem.* **1995,** *60,* 1990–1998. (c) O'Hair, R. A. J.; Freitas, M. A.; Williams, T. D. *J. Org. Chem.* **1996,** *61,* 2374–2382. (d) Freitas, M. A.; O'Hair, R. A. J.; Dua, S.; Bowie, J. H. *Chem. Commun.* **1997,** 1409–1410.
2. Reid, G. E.; Simpson, R. J.; O'Hair, R. A. J. *J. Am. Soc. Mass Spectrom.* **1998,** *9,* 945–956.
3. Ab initio studies when combined with experimental work can provide useful insights into the sites of protonation in simple peptides: (a) Wu, J.; Lebrilla, C. B. *J. Am. Chem. Soc.* **1993,** *115,* 3270–3275. (b) Wu, J.; Lebrilla, C. B. *J. Am. Soc. Mass Spectrom.* **1995,** *6,* 1165–1174. (c) Zhang, K.; Zimmerman, D. M.; Chung-Phillips, A.; Cassady, C. J. *J. Am. Chem. Soc.* **1993,** *115,* 10812–10822. (d) Zhang, K.; Cassady, C. J.; Chung-Phillips, A. *J. Am. Chem. Soc.* **1994,** *116,* 11512–11521; (e) Cassady, C. J.; Carr, S. R.; Zhang, K.; Chung-Phillips, A. *J. Org. Chem.* **1995,** *60,* 1704–1712.
4. For fragmentation reactions of protonated amino acids see: (a) Kulik, W.; Heerma, W. *Biomed. Mass Spectrom.* **1988,** *15,* 419–427. (b) Dookeran, N. N.; Yalcin, T.; Harrison, A. G. *J. Mass Spectrom.* **1996,** *31,* 500–508.

5. Uggerud, E. *Theor. Chim. Acta* **1997,** *97*, 313–316.
6. For fragmentation reactions of protonated dipeptides see: (a) Pelzer, G.; Duchateau, P.; Natalis, P.; De Pauw, E. *Spectroscopy* **1987,** *5*, 149–156. (b) Kulik, W.; Heerma, W. *Biomed. Mass Spectrom.* **1988,** *17*, 173–180. (c) Isa, K.; Omote, T.; Amaya, M. *Org. Mass Spectrom.* **1990,** *25*, 620–628. (d) Cordero, M. M.; Wesdemiotis, C. *Org. Mass Spectrom.* **1993,** *28*, 1041–1046.
7. For fragmentation reactions of protonated tripeptides see: (a) Kulik, W.; Heerma, W. *Biomed. Mass Spectrom.* **1989,** *18*, 910–917. (b) Cordero, M. M.; Wesdemiotis, C. *Org. Mass Spectrom.* **1994,** *29*, 382–390. (c) Morgan, D. G.; Bursey, M. M. *Org. Mass Spectrom.* **1994,** *29*, 354–359. (d) Morgan, D. G.; Bursey, M. M. *Org. Mass Spectrom.* **1995,** *30*, 290–295. (e) Yalcin, T.; Khouw, C.; Csizmadia, I. G.; Pererson, M. R.; Harrison, A. G. *J. Am. Soc. Mass Spectrom.* **1995,** *6*, 1165–1174. (f) Klassen, J. S.; Kebarle, P. *J. Am. Chem. Soc.* **1997,** *119*, 6552–6563; (g) Nold, M. J.; Wesdemiotis, C.; Yalcin, T.; Harrison, A. G. *Int. J. Mass Spectrom. Ion Processes* **1997,** *164*, 137–153.
8. (a) Dongre, A. R.; Jones, J. L.; Somogyi, A.; Wysocki, V. H. *J. Am. Chem. Soc.* **1996,** *118*, 8365–8374. (b) Harrison, A. G.; Yalcin, T. *Int. J. Mass Spectrom. Ion Processes* **1997,** *165/166*, 339–347.
9. Maycock, C. D.; Stoodley, R. J. *J. Chem. Soc., Pekin Trans. I* **1979,** 1852–1857.
10. Busch, K. L.; Glish, G. L.; McLuckey, S. A. *Mass Spectrometry/Mass Spectrometry. Techniques & Applications of Tandem Mass Spectrometry*; VCH: New York, 1988.
11. Gamess Ver 31 Oct 1996, Iowa State University, Schmidt, M. W.; Baldridge, K. K.; Boatz, J. A.; Elbert, S. T.; Gordon, M. S.; Jensen, J. H.; Koseki, S.; Matsunaga, N.; Nguyen, K. A.; Su, S. J.; Windus, T. L.; Dupuis, M.; Montgomery, J. A. *J. Comput. Chem.* **1993,** *14*, 1347–1363.
12. Gaussian 94, Frisch, M. J.; Gill, P. M. W.; Wong, M. W.; Head-Gordon, M.; Trucks, G. W.; Foresman, J. B.; Schlegel, H. B.; Raghavachari, K.; Robb, M.; Johnson, B. G.; Gonzalez, C.; Defrees, D. J.; Fox, D. J.; Replogle, E. S.; Gomperts, R.; Andres, J. L.; Martin, R. L.; Baker, J.; Stewart, J. J. P.; Pople, J. A. 1994, Gaussian Inc., Pittsburgh PA, USA.
13. Spartan Ver 5.0., Wavefunction, Inc., 18401 Von Karman Avenue, Suite 370, Irvine, CA 92612.
14. Hehre, W. J.; Pople, J. A.; Radom, L. *Ab Initio Molecular Orbital Theory*; Wiley: New York, 1986.
15. Reid, G. E.; Simpson, R. J. *Anal. Biochem.* **1992,** *200*, 301–309.
16. Scott, A. P.; Radom, L. *J. Phys. Chem.* **1996,** *100*, 16502–16513.
17. (a) Capon, B. *Q. Rev.* **1964,** *18*, 45–111. (b) March, J. *Advanced Organic Chemistry, 4th ed.*; Wiley: New York, 1992, pp 308–312.
18. For ab initio calculations on related carbocation systems see: (a) Rodriquez, C. F.; Hopkinson, A. C. *J. Mol. Struct.* **1987,** *152*, 69–81. (b) Bertone, M.; Vuckovic, D. L.; Cunje, A.; Rodriquez, C. F.; Lee-Ruff, E.; Hopkinson, A. C. *Can. J. Chem.* **1995,** *73*, 1468–1477.
19. It is interesting to note that the main features (key C–S and C–C bond lengths and an imaginary frequency of 420i cm^{-1}) of this transition state resemble those for the anionic displacement of HS^- from $HSCH_2CH_2S^-$. Gronert, S.; Lee, J. M. *J. Org. Chem.* **1995,** *60*, 6731–6736.
20. For an excellent review on the role of ion–molecule complexes see: Bowen, R. D. *Acc. Chem. Res.* **1991,** *24*, 364–371.
21. For a discussion on how the different collision conditions can effect the lifetime of ion–molecule complexes, and how this relates to the observation of fragment ions in protonated amides see: Tu, Y. P.; Harrison, A. G. *J. Am. Soc. Mass Spectrom.* **1998,** *9*, 454–462.
22. Johnson, R. S.; Krylov, D.; Walsh, K. A. *J. Mass Spectrom.* **1995,** *30*, 386–387.
23. (a) Speir, J. P.; Amster, I. J. *J. Am. Soc. Mass Spectrom.* **1995,** *6*, 1069–1078. (b) Price, W. D.; Williams, E. R. *J. Phys. Chem. A* **1997,** *101*, 8844–8852.
24. (a) Ballard, K. D.; Gaskell, S. J. *J. Am. Soc. Mass Spectrom.* **1993,** *4*, 477–481. (b) Schnier, P. D.; Price, W. D.; Jockusch, R. A.; Williams, E. R. *J. Am. Chem. Soc.* **1996,** *118*, 7178–7189.
25. For discussions on the role of various amino acid residues on the formation of sequence ions in the high energy CID MS/MS spectra of peptide $[M+H]^+$ ions see: (a) Papayannopoulos, I. A. *Mass. Spectrom. Rev.* **1995,** *14*, 49–73. (b) van Dongen, W. D.; Ruijters, H. F. M.; Luinge, H.-J.; Heerma, W.; Haverkamp, J. *J. Mass Spectrom.* **1996,** *31*, 1156–1162.
26. For sequence ion nomenclature see: (a) Roepstorff, P.; Fohlman, J. *Biol. Mass. Spectrom.* **1994,** *11*, 601. (b) Papayannopoulos, I. A.; Biemann, K. *Acc. Chem. Res.* **1994,** *27*, 370–378.
27. (a) Schwartz, B. L.; McClain, R. D.; Erickson, B. W.; Bursey, M. M. *Rapid Commun. Mass Spectrom.* **1993,** *7*, 339–342. (b) Summerfield, S. G.; Whiting, A.; Gaskell, S. J. *Int. J. Mass Spectrom. Ion Processes* **1997,** *162*, 149–161. (c) Loo, J. A.; He, J. X.; Cody, W. L. *J. Am. Chem. Soc.* **1998,** *120*, 4542–4543.
28. Yu, W.; Vath, J. E.; Huberty, M. C.; Martin, S. A. *Anal. Chem.* **1993,** *65*, 3015–3023.
29. Yalcin, T.; Harrison, A. G. *J. Mass Spectrom.* **1996,** *31*, 1237–1243.